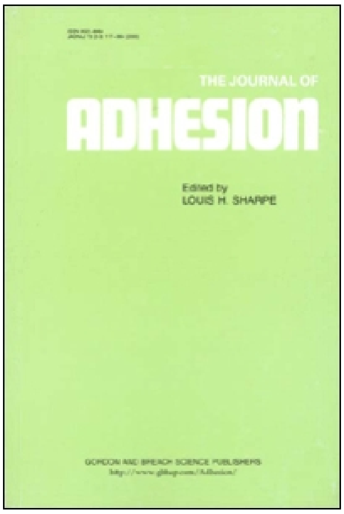

The Journal of Adhesion
Publication details, including instructions for authors and subscription information:
http://www.informaworld.com/smpp/title~content=t713453635

An Elementary Plate Theory Prediction for Strain Energy Release Rate of the Constrained Blister Test

Yeh-Hung Lai[a]; David A. Dillard[a]
[a] Engineering Science and Mechanics Department, Virginia Polytechnic Institute and State University, Blacksburg, Virginia, U.S.A.

To cite this Article Lai, Yeh-Hung and Dillard, David A.(1990) 'An Elementary Plate Theory Prediction for Strain Energy Release Rate of the Constrained Blister Test', The Journal of Adhesion, 31: 2, 177 — 189
To link to this Article: DOI: 10.1080/00218469008048223
URL: http://dx.doi.org/10.1080/00218469008048223

J. Adhesion, 1990, Vol. 31, pp. 177–189
Reprints available directly from the publisher
Photocopying permitted by license only

Printed in the United Kingdom

An Elementary Plate Theory Prediction for Strain Energy Release Rate of the Constrained Blister Test

YEH-HUNG LAI and DAVID A. DILLARD

Engineering Science and Mechanics Department, Virginia Polytechnic Institute and State University, Blacksburg, Virginia 24061, U.S.A.

(Received October 12, 1988; in final form November 19, 1989)

A technique based on elementary plate theory is proposed for estimating the strain energy release rate of the constrained blister specimen for the case of a relatively stiff blister adherend. The results of finite element analysis for an aluminum specimen confirm the applicability of the elementary plate theory approach for the constrained blister test. The paper also proposes an experimental scheme which could be automated to measure the necessary parameters to determine the strain energy release rate of the constrained blister specimen.

KEY WORDS Blister test; constrained blister test; stress analysis; contact problem; plate theory; strain energy release rate; fracture mechanics.

INTRODUCTION

Over the years, a large number of test geometries have been devised for evaluating the properties of *in situ* adhesives. Among these tests, the blister specimen originally proposed by Williams[1] offers an attractive approach for studying environmental exposure because the diffusion occurs nearly perpendicular to the debond, avoiding lateral problems present in double cantilever beam type specimens.[2] Also, because of the axisymmetric nature of the blister specimen, the non-uniformity of the stress field along the debond front is much less than for a finite width specimen. Anderson, *et al.*[3] discuss closed form and numerical solutions for the strain energy release rate for the blister test, and have identified regions of applicability for formulae for a penny-shaped crack between two semi-infinite media and for elementary plate theory. Gent and Lewandowski[4] presented an approximate solution for the case of a very thin blister adherend in which membrane stiffness is significantly larger than the bending stiffness. Allen and Senturia discussed the case of thin films in the blister test for annular and rectangular shapes with and without residual stresses.[5,6] Although these approaches suggest the applicaiblity of the blister test for a wide range of materials and geometries, several problems exist. In the blister test, the strain energy release rate is always an increasing function of debond radius, resulting in non-stable debonding under constant pressure loading. Furthermore, in these approaches, the mode I to mode II ratio changes as debond radius increases, complicating the analysis of the experimental results. Recently, a novel modification of the blister test called the constrained blister test (Figure 1) that permits nearly constant strain energy release rate testing of adhesive bonds with nearly constant mode mix was proposed independently by Dillard and Chang[7,8] and Napolitano, *et al.*[9] By placing a flat constraint above the blister to limit its deformation (Figure 1), the volume displaced is approximately proportional to the debond area. This results in a nearly constant strain energy release rate test. An approximate solution of strain energy release rate proposed by Dillard and Chang[7,8] is

$$G_c = p_c h q \tag{1a}$$

where G_c is the critical value of the strain energy release rate and may be a function of debond rate and environment, p_c is the debonding pressure in the blister, h is the constraint height, and q is the correction factor.

If one makes the assumption that the suspended region may be approximated by a straight line, q takes on the form:

$$q = \left(1 - \frac{d}{2a}\right) + \left(\frac{d}{3a} - \frac{1}{2}\right)\frac{\partial d}{\partial a} \tag{1b}$$

where a is the debond radius, and d is the length of the suspended region.

A series of tests on adhesive tapes showed that a state of nearly constant G was obtained.[7,8] Numerical analyses by Lai and Dillard[10] confirmed the applicability of the approximate solution, Eq. (1), for several typical cases. The numerical analyses also suggested that the measurements of the length of the suspended region, d, and debond radius, a, are always required in order to determine accurately the correction factor, q and, therefore, G. For thin films or soft specimens, a and d can be easily measured by taking pictures through a

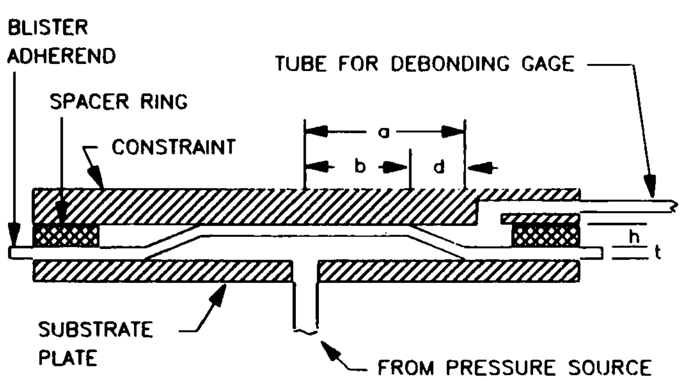

FIGURE 1 Configuration of the constrained blister test.

transparent upper constraint. However, in tests with a stiff specimen such as aluminum, high pressure is required and a rigid opaque constraint such as thick aluminum or steel is needed. In these cases, values of a and d cannot be readily obtained. Thus, an alternate technique that can predict strain energy release rate without measuring a and d is developed, and can be used in lieu of the numerical analysis[10] for obtaining the total strain energy release rate.

THE APPLICATION OF ELEMENTARY PLATE THEORY TO PREDICT STRAIN ENERGY RELEASE RATE

Several energy balance formalisms have been proposed for determining strain energy release rates for adhesive bonds. The approach used here is based on the classical energy conservation approach where localized viscoelastic and plastic deformations in the vicinity of the crack tip are included in the critical strain energy release rate, $G_c = G_c(da/dt)$, making it a function of debond rate. The choice to include this near-field energy dissipation in the G_c term provides expediency, and has been discussed by Knauss,[11] Williams,[12] and used by Anderson, *et al.*[3] and others.[13,14] This is a reasonable approach since near-field dissipation cannot readily be separated from an "inherent" surface energy anyway. When debonding occurs,

$$G_c\,\delta A = \delta W - \delta U - \delta Z \tag{2}$$

where G_c is the critical value of strain energy release rate and may be a function of debond rate and environment, δA is the variation of the debond area, δW is the variation in work done on the system, δU is the variation of the strain energy of the specimen, and δZ is the variation of the energy dissipated in the region away from the vicinity of the debond tip, which may include viscoelastic, frictional effects, and plastic dissipation.

In the constrained blister test with an elastic specimen, one may neglect the energy dissipation due to far-field viscoelastic effects. In the test, one may also view the specimen as a thin, flat, circular plate subjected to small deformations, which is the case for a relatively stiff specimen constrained to a small constraint height. Thus, the displacement in the radial direction is negligible and one may neglect the slipping and the dissipated frictional energy between the specimen and the upper constraint. (Numerical results also confirm that even if frictional slipping occurs against the constraint, the effect on the energy balance is negligible.[10]) Furthermore, if the plastic zone is small compared with the crack length and is localized to the crack tip, which is shown in Ref. 10 for an aluminum specimen, one can neglect the dissipated plastic energy. Under the above conditions, the δZ term in Eq. (2) can be neglected. The strain energy release rate, G, will be expressed as energy released due to the variation of the debond area and is given by:

$$G = p\frac{\partial V}{\partial A} - \frac{\partial U}{\partial A} \tag{3}$$

where V is the volume of the blister, and p is the pressure.

Although assumed negligible in earlier work,[7,8,9] the variation in strain energy is retained in the present analysis, although only bending strain energy is considered in the following closed form analysis.

If the thickness of the specimen is small in comparison with its radius ($t \le \frac{1}{5}a$) and the deflection is small compared with its thickness ($w \le t$), elementary plate theory can be used and the deflection is given as:[15,16]

$$w(r) = C_1 + C_2 \ln r + C_3 r^2 + C_4 r^2 \ln r + \frac{pr^4}{64D} \tag{4}$$

where $w(r)$ is the deflection of the mid surface of plate at any radial position, r, C_1, C_2, C_3 and C_4 are undetermined constants, p is the uniformly distributed pressure and D is the bending rigidity which is given as

$$D = \frac{Et^3}{12(1 - \nu^2)},$$

where t is the thickness of the specimen, E is the Young's modulus, and ν is the Poisson's ratio.

In the case of a constrained blister, we assume that the edge of the blister is clamped. In order to determine the four unknown constants and the unknown radius of the inner edge of suspended region, b, two boundary conditions are applied at the debond radius, a:[15]

$$(w)_{r=a} = 0, \tag{5a}$$

$$\left(\frac{dw}{dr}\right)_{r=a} = 0, \tag{5b}$$

and three at the inner edge of suspended region of radius b:

$$(w)_{r=b} = h, \tag{5c}$$

$$\left(\frac{dw}{dr}\right)_{r=b} = 0, \tag{5d}$$

$$(M)_{r=b} = 0, \tag{5e}$$

where the last boundary conditon, Eq. (5e), is based on the assumption that just inside the circle of radius b the slope is zero, therefore, the bending moment must also be zero along this circle, since the inner portion of the plate remains flat.

Thus, a system of five nonlinear equations is obtained to determine the unknown constants and b:

$$C_1 + C_2 \ln a + C_3 a^2 + C_4 a^2 \ln a = -\frac{pa^4}{64D} \tag{6a}$$

$$C_1 + C_2 \ln b + C_3 b^2 + C_4 b^2 \ln b = -\frac{pb^4}{64D} + h \tag{6b}$$

$$C_2\frac{1}{a} + C_3(2a) + C_4a(2\ln a + 1) = -\frac{pa^3}{16D} \quad \text{(6c)}$$

$$C_2\frac{1}{b} + C_3(2b) + C_4b(2\ln b + 1) = -\frac{pb^3}{16D} \quad \text{(6d)}$$

$$C_2\frac{\nu - 1}{b^2} + 2C_3(\nu + 1) + C_4(3 + 2\ln b + 2\nu\ln b + \nu) = -\frac{pb^2}{16D}(3 + \nu) \quad \text{(6e)}$$

From Ref. 11, the strain energy due to bending can be expressed as:

$$U = \frac{D}{2}\int_b^a \left\{\left[\frac{\partial^2 w}{\partial r^2} + \frac{1}{r}\frac{\partial w}{\partial r}\right]^2 - 2(1-\nu)\left[\frac{\partial^2 w}{\partial r^2}\right]\left[\frac{1}{r}\frac{\partial w}{\partial r}\right]\right\}dr \quad (7)$$

and the volume of the blister is

$$V = \pi(a-d)^2h + \int_{a-d}^{a} 2\pi r w(r)\, dr \quad (8)$$

Theoretically, by substituting Eq. (4) into Eq. (7) and Eq. (8), differentiating U and V with respect to A and then substituting into Eq. (3), we can obtain the strain energy release rate, G. However, Eq. (6) is a system of nonlinear equations; obtaining the solutions in explicit form for the unknown constants and b is impractical. Consequently, calculating the strain energy release rate numerically is a more practical approach. Fortunately, the numerical library to solve a system of nonlinear equations and do numerical integration is easy to obtain for either a personal or main frame computer.

In the current study, Eq. (6) is solved by using the IMSL[17] subroutine ZSPOW; the bending strain energy, U, and the volume of blister, V, are integrated using subroutine DCADRE. By imposing a small variation δa on debond radius, the quantities δV, δA and δU are readily obtained. Substituting these quantities into Eq. (3), we can then obtain the strain energy release rate numerically.

In the following section, the predictions of strain energy release rate based on the above algorithm will be compared with finite element predictions for aluminum adherend cases. A simple experimental procedure will also be proposed to predict the strain energy release rate by using this algorithm. The analysis of the constrained blister test based on this algorithm will also be compared with the regular blister test to clarify their differences.

RESULTS AND DISCUSSIONS

Figures 2 to 5 are the predictions of the plate theory compared with those of finite element analysis with the geometrically nonlinear option for an aluminum 6061-T6 specimen which has a thickness of 3 mm, a constraint height of 2 mm, and is subjected to a pressure of 200 kPa. The finite element program called

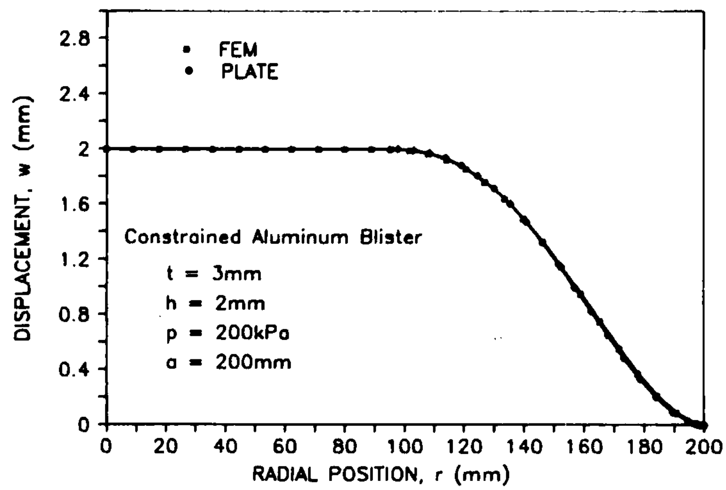

FIGURE 2 Profiles of an aluminum specimen for the analyses of FEM and plate theory.

ABAQUS, which is capable of handling contact problems, was used (version 4-7-1). In these figures, the legends denoted 'FEM' and 'PLATE', represent the predictions of finite element analysis and elementary plate solution, respectively.

Figure 2 illustrates a typical deformed profile at the midplane of the specimen for an aluminum specimen of $a = 200$ mm. Excellent agreement is seen between the predictions of the geometrically nonlinear finite element analysis and elementary plate theory. It should be noted that according to Ref. 15, if there were no upper constraint, the deflection of a plate of the same geometry subjected to this loading condition would be so large that the problem would need to be treated as a large deformation plate problem and the deviation of deflection at the center from elementary plate theory with respect to that from an approximate solution of large deflection plate theory would be around 400%. The excellent agreement in Figure 2 shows that the upper constraint has prevented membrane effects from significantly stiffening the plate. The elementary plate theory solution which ignores membrane effects agrees very well with the finite element solution which accounted for geometric nonlinearities.

Figure 3 illustrates the stress distribution in the radial direction at both the top and bottom surface of the specimen. It should be noted that the stress distributions from both elementary plate theory and finite element analysis do not exceed the yielding point except for the region very near the crack front which has a singular point (plastic zone is about 0.05% of the thickness). It is seen that the stresses from the elementary plate theory are higher than those of the finite element analysis in the suspended region. In the contact region, however, the stresses from the elementary plate theory are smaller. The reason for the former phenomenon is due to the assumption that the outer edge is fixed at $r = a$ in the elementary plate approach, which provides a stiffer constraint than exists in the real specimen analyzed in the finite element model, and thus causes

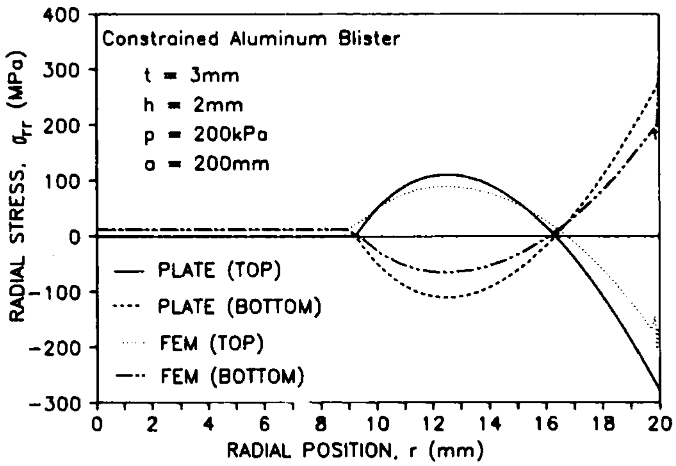

FIGURE 3 Radial stress distributions predicted by FEM and plate theory along the top and bottom surfaces in the radial direction of an aluminum specimen.

higher bending moment and stresses. The reason for the latter phenomenon is due to the assumption of the small deformation for the elementary plate theory which results in zero stresses at the mid-plane of the specimen, where the finite element analysis shows non-zero membrane stresses. Although the predicted stresses deviate substantially, it will be shown that the stored energy is small in comparison to input work, thereby minimizing errors in predicted strain energy release rates.

Although the finite element results did not show an oscillation of displacements near $r = b$, a small oscillation of the stress distribution in the r direction, σ_{rr}, did reveal that very localized oscillation occurs.[10] However, the excellent agreement of the displacement profile suggests that $(M)_{r=b} = 0$ is a good assumption as well as the fixed end assumption at $r = a$.

Figure 4 illustrates the volume of the blister *versus* debond radius. Excellent agreement is seen. For $a < 102$ mm, the elementary plate solution indicates that the specimen does not touch the upper constraint and suggests that initial debond radius in the constrained blister test should be larger than 102 mm.

Figure 5 illustrates the strain energy release rates *versus* a, using the results from the finite element analysis, approximate solution, Eq. (1a), and elementary plate theory. The variation of input work on the system and the variation of strain energy from Eq. (3), based on elementary plate theory, are also shown in the figure to indicate the relative magnitude of the bending strain energy. The legends, 'G-PLATE', '$G = phq$', and 'FEM', represent the energy release rates obtained from the elementary plate theory, approximate solution by Dillard, *et al.*[7,8] and the finite element analysis, respectively. The other two legends, 'dW/dA-PLATE' and 'dU/dA-PLATE', represent the variation of the work on the system and the variation of the strain energy of the specimen from the elementary plate thoery, respectively. The calculations were performed at a strain

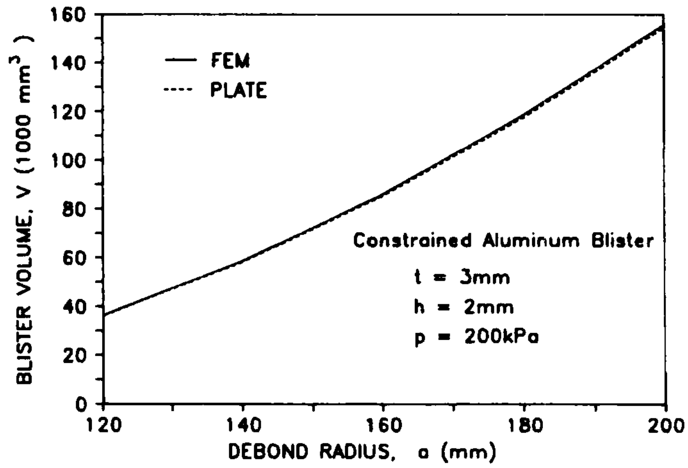

FIGURE 4 Volume of the blister *versus* debond radius predicted by FEM and plate theory for an aluminum specimen.

energy release rate which is typical for aluminum epoxy bonding.[3] Two paths were considered for the finite element analysis. One is the path whereby the specimen is lifted to contact the upper constraint by the applied pressure; the other path is for the blister first unconstrained and then the rigid upper constraint moved down until the final configuration is the same. In both analyses, the coefficient of friction varies from 0 to 0.5. It was found that the difference between the paths is less than 0.5%, for all cases, which suggests that the contact condition does not induce large error for the energy balance equation, Eq. (2). It is noted that the strain energy release rates from the elementary plate theory are

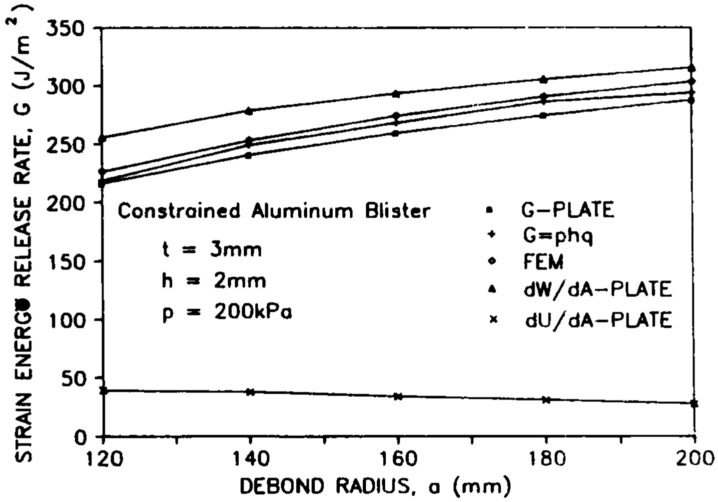

FIGURE 5 Strain energy release rates *versus* debond radius for an aluminum specimen.

smaller than the FEM predictions. The difference appears to arise because the analytical solution predicts higher stresses, as shown in Fig. 3, and thus, variation in strain energy, $\partial U/\partial A$, than the FEM results. However, in Ref. 8, it was shown that the variation of the strain energy is only a small fraction of the variation of the input work. Thus, the error from the stress prediction does not induce a large error when the total strain energy release rate is calculated, because the first term on the right hand side of Eq. (3), $p(\partial V/\partial A)(=\partial W/\partial A)$, is the dominant term and is shown to be very accurate from the volume prediction from the elementary plate theory in Fig. 4. It is also seen in this figure that the approximate solution, $G=phq$, is a good approach if one can obtain the debond radius and the length of the suspended region, which are obtained from the finite element results in the current comparisons. All three approaches show that the rate of increase of G decreases as debonding proceeds, and a nearly constant G is seen at large values of debond radius.

Figures 4 and 5 also offer us an efficient way to predict the debond radius and the strain energy release rate in a constrained blister test. The prediction procedures are illustrated in Fig. 6 and stated as follows: First of all, use the algorithm developed in the previous section to run several cases for different parameters such as p, h, t, and a for the selected specimen geometries to determine the conditions for the existence of contact between the specimen and upper constraint. Secondly, run several cases with different a's to obtain the

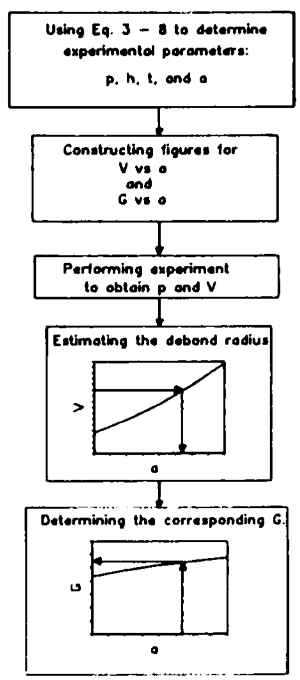

FIGURE 6 The automated algorithm to determine G.

figures of "volume *vs* a" and "G *vs* a". Thirdly, perform the experiment with the initial debond size predicted from step 1 and measure the blister volume. Finally, from the figure of "volume *vs* a", one can determine the debond size and refer to the figure of "G *vs* a" to obtain the G for the specific a's. Using these procedures, the strain energy release rate is easily determined and automated evaluation is possible.

Although the theoretical background of the current approach is confined to small deformation plate theory, it is reasonable that if the loading condition and specimen geometry result in a small length for the suspended region, the error for volume predictions between elementary plate approach and nonlinear finite element analysis would be small even for the constraint height larger than the blister thickness. Since the variation of input work is the dominant term determining the strain energy release rate,[8] the error induced from the increasing membrane strain energy may be still relatively small when determining the total strain energy release rate. Because a nondimensionalized and explicit form solution of the constrained blister test could not be obtained in the current study, the complete criterion of the applicability of the elementary plate theory for the constrained blister test could not be established. However, by increasing the constrained height, h, beyond the limitation of the small deformation plate theory, one can obtain a greater understanding of the limitations of the proposed approach. Figure 7 illustrates the strain energy release rate *versus* constraint height for both geometrically nonlinear finite element analysis and the elementary plate approach for the same aluminum specimen analyzed previously. The applied pressure is 1 MPa. It is seen that the prediction of G from plate theory has only 5.3% deviation even for an h which is four times the adherend thickness. It should be noted that at $h = 5t$ for this geometry, the specimen does not touch

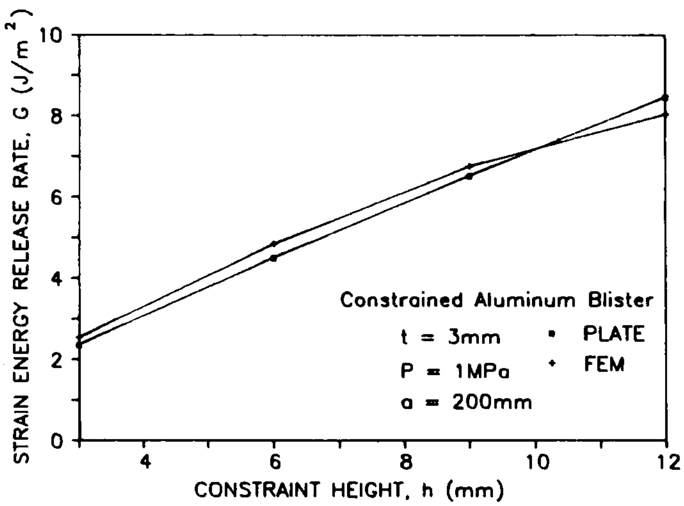

FIGURE 7 Strain energy release rates *versus* constraint height predicted by FEM and plate theory for an aluminum specimen.

the upper constraint, thus no further comparison is shown in the figure. It is also seen that the rate of change of G obtained from FEM predictions decreases as h increases, while that from plate theory does not. This suggests that the membrane effect increases as h increases and larger deviation is expected for $h > 4t$.

Although Figure 7 shows that the strain energy release rate is still accurate when h is four times the thickness, the predictions of the blister volume are not as accurate as those of strain energy release rate. Figure 8 shows the volume of the blister *versus* the constraint height. It is seen that the accuracy of volume prediction decreases as h increases, which is due to the increase of the membrane effect considered by the FEM analysis. As $h = 3t$, the deviation of the volume prediction from the plate theory is about 12% from the FEM analysis. It is noted that the strain energy release rate predictions have higher accuracy than volume predictions. The phenomenon can be explained in that even though the accuracy of the volume predictions decrease for larger h, the variations of the volume are about the same from the elementary plate and FEM predictions under a small increment of debond radius, δa, and thus results in better prediction for the variation of input work and the strain energy release rate.

Figure 9 illustrates the variation of the strain energy release rate based on plate theory as the debond grows for the same aluminum specimen as in Figs 2–5. The variations of work input on the system and strain energy as the debond grows are also illustrated. The results from the regular blister test and constrained blister test are noted as '−BT' and '−CBT' in the figure. When a is smaller than 102 mm, the deflection at the center of the plate calculated from elementary plate theory:[11]

$$w = \frac{1}{64}\frac{p}{D}a^4 \tag{9}$$

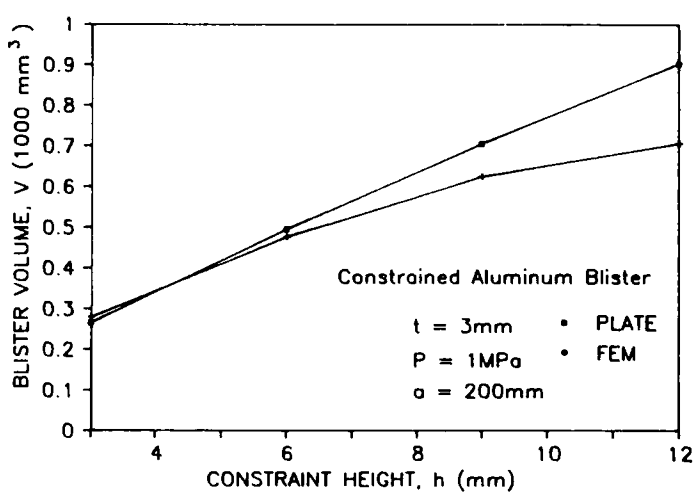

FIGURE 8 Volume of the blister *versus* constraint height predicted by FEM and plate theory for an aluminum specimen.

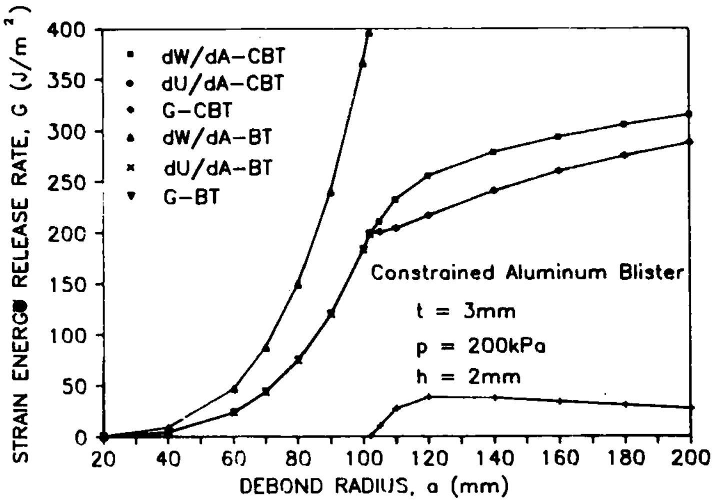

FIGURE 9 Illustration for the variation of G during the debonding process for a constrained blister test with a regular blister as a is smaller than 102 mm.

is smaller than the constraint height, and the radius of the contact region, b, calculated from Eq. (6) is smaller than 0. Both results show that the specimen does not touch the upper constraint. On the other hand, for $a > 102$ mm, both results indicate that the specimen contacts the upper constraint. Thus, for $a < 102$ mm, the specimen is a regular blister and the strain energy release rate is calculated from Eq. (4) which has

$$\frac{\partial U}{\partial A} = \frac{1}{2} p \frac{\partial V}{\partial A}$$

and thus:[11]

$$G = \frac{3}{32} \frac{(1-\nu^2)}{Et^3} p^2 a^4. \tag{10}$$

It is clearly seen that for $a < 102$ mm, G is a function of a^4 and small errors of measuring debond radius would cause large errors in G. For $a > 102$ mm, the specimen becomes a constrained blister and G is calculated from the approach proposed in the previous section. It is seen that small errors in measuring or estimating debond radius would not induce the large errors in G as would the regular blister test. It is also seen that the variation of the strain energy term in Eq. (4) is more important in the regular blister approach, while it is less important in the constrained blister approach. This is discussed in some detail in Ref. 8.

CONCLUSIONS

An approach based on elementary plate theory to evalutate the strain energy release rate in the constrained blister test is proposed in this paper. This approach is especially applicable for relatively stiff blister specimens, such as metallic specimens, which would cause difficulty determining the debond radius and contact region by observing through the transparent upper constraint in the test. The strain energy release rates predicted from this approach are in good agreement with those predicted from the finite element analysis and the previously-proposed approximate solution. In contrast to the rapid increase of the strain energy release rate predicted by the free blister test, a nearly constant strain energy release rate during the debonding process is predicted from this approach. Although elementary plate theory is applicable for the maximum deflection smaller than the thickness of the plate, the results of an aluminum specimen suggest that under the appropriate loading and geometrical conditions, the proposed approach is applicable for cases with the constraint height larger than the specimen thickness.

In the experimental scheme of the constrained blister test proposed in this paper, only the volume and the pressure difference between the inside and outside of the blister need to be measured during the debonding process. The measurements are easy to perform and may be automated. Thus, this approach offers a practical and efficient way to estimate strain energy release rate for metal adherends and suggests wider applicability of the constrained blister technique.

Acknowledgements

The authors would like to acknowledge the finanical support of Texas Research Institute, Inc. (Dr. J. S. Thronton), the Virginia Center for Innovative Technology (Dr. C. Spencer), and the Office of Naval Research (Dr. L. Peebles). We are also grateful to Yeou Shin Chang for his helpful comments.

References

1. M. L. Williams, *Journal of Applied Polymer Science* **13**, 9–40 (1969).
2. D. R. Lefebvre, D. A. Dillard and H. F. Brinson, *Experimental Mechanics* **28**, 38–44 (1988).
3. G. P. Anderson, S. J. Bennett and K. L. DeVries, *Analysis and Testing of Adhesive Bonds* (Academic Press, New York, 1977).
4. A. N. Gent and L. H. Lewandowski, *J. Appl. Polym. Science* **33**, 1567–1577 (1987).
5. M. G. Allen and S. D. Senturia, *Proc of the ACS Div. of Polymer Materials: Science and Engineering* **56**, 735–739 (1987).
6. M. G. Allen and S. D. Senturia, *J. Adhesion* **25**, 305–315 (1988).
7. D. A. Dillard and Y. S. Chang, *VPI Report* #VPI-E-87-24, Blacksburg, Virginia, 1987.
8. Y. S. Chang, Y. H. Lai, and D. A. Dillard, *J. Adhesion* **27**, 197–211 (1989).
9. M. J. Napolitano, A. Chudnovskyc and A. Moet, *ACS Div. of PMSE Preprints* **57**, 755–759 (1987).
10. Y. H. Lai and D. A. Dillard, "Numerical analysis of the constrained blister test", *J. Adhesion,* in review.
11. W. G. Knauss, *Intern. J. Fracture Mechanics* **6**, 7–20 (1970).
12. M. L. Williams, *Intern. J. Fracture Mechanics* **1**, 292–310 (1965).
13. W. S. Blackburn, *Intern. J. Fracture Mechanics* **7**, 354–356 (1971).
14. M. F. Kanninen, in *Prospects of Fracture Mechanics,* G. C. Sih, Ed. (H. C. van Elst, D. Broek, Noordhoff, 1974).
15. S. Timoshenko and S. Woinowsky-Krieger, *Theory of Plates and Shells* (McGraw Hill, New York, 1959).
16. R. Szilard, *Theory and Analysis of Plates* (Prentice-Hall, Englewood Cliffs, NJ, 1974).
17. IMSL, The International Mathematics Subroutine Library, IMSL, INC, 1987.